
TURB-HEL: AN OPEN-ACCESS DATABASE OF HELICALLY FORCED HOMOGENEOUS AND ISOTROPIC TURBULENCE

A PREPRINT

Luca Biferale

Dept. Physics and INFN
University of Rome Tor Vergata and INFN, Italy
biferale@roma2.infn.it

F. Bonaccorso

Dept. Physics and INFN
University of Rome Tor Vergata, Italy.
fabio.bonaccorso@roma2.infn.it

Moritz Linkmann

School of Mathematics and Maxwell Institute for
Mathematical Sciences
University of Edinburgh, UK
moritz.linkmann@ed.ac.uk

Damiano Capocci

Dept. Physics and INFN
University of Rome Tor Vergata, Italy.
damiano.capocci@roma2.infn.it

April 12, 2024

ABSTRACT

We present TURB-Hel, a database formed by two datasets of incompressible homogeneous and isotropic turbulence, maintained in a statistically stationary state by fully helical forcing. The aim is to provide a dataset that clearly exhibits the phenomenon of the helicity cascade from the large to the small scales generated by a large-scale forcing that breaks the mirror symmetry. This database offers the possibility to realize a wide variety of analyses of fully developed turbulence from the sub-grid scale filtering up to the validation of an *a posteriori* LES.

TURB-Hel is available for download using the SMART-Turb portal <http://smart-turb.roma2.infn.it>.

1 Introduction

Kinetic helicity, the correlation between velocity fluctuations, \mathbf{u} , and vorticity fluctuations, $\boldsymbol{\omega}$, is known to influence turbulent dynamics and coherent structures formation Waleffe (1992) (other references) and to be connected to the breaking of the symmetry under inversion of all axes in a rotationally invariant ensemble.

High levels of helicity have been associated with: a strong depletion of the kinetic energy fluxes across scales Kraichnan (1973) as a consequence of the nonlinearity reduction caused by the alignment of velocity and vorticity and with low dissipation regions Moffatt (2014). Like energy, helicity is a quadratic invariant of the Euler equations but, unlike energy, it is not sign definite. In this respect, the interactions between helical Fourier modes of opposite signs (heterochiral sector) contribute to the energy transfer from large to small scales Waleffe (1992) Alexakis & Biferale (2018) Alexakis (2017) while those with the same sign (homochiral sector) are responsible for the inverse energy transfer across scales in the inertial range Biferale *et al.* (2012), Biferale *et al.* (2013), Sahoo *et al.* (2015).

Any solenoidal vector field can be decomposed into positively and negatively helical components Waleffe (1992). That is, the velocity field can be written as

$$\mathbf{u}(\mathbf{x}, t) = \mathbf{u}^+(\mathbf{x}, t) + \mathbf{u}^-(\mathbf{x}, t). \quad (1)$$

The fields \mathbf{u}^+ and \mathbf{u}^- are obtained by projecting the Fourier coefficients $\hat{\mathbf{u}}(\mathbf{k}, t)$ onto basis vectors which are eigenfunctions of the curl operator in Fourier space

$$\hat{\mathbf{u}}^\pm(\mathbf{k}, t) = u^\pm(\mathbf{k}, t) \mathbf{h}^\pm(\mathbf{k}), \quad (2)$$

where $i\mathbf{k} \times \mathbf{k} \mathbf{h}^\pm(\mathbf{k}) = \pm \mathbf{h}^\pm(\mathbf{k})$. The total kinetic helicity can then be calculated as

$$\langle \mathbf{u}(\mathbf{x}, t) \cdot \boldsymbol{\omega}(\mathbf{x}, t) \rangle_V = \sum_{\mathbf{k}} \hat{\mathbf{u}}(\mathbf{k}, t) \cdot \hat{\boldsymbol{\omega}}(\mathbf{k}, t) = \sum_{\mathbf{k}} k (u^+(\mathbf{k}, t)^2 - u^-(\mathbf{k}, t)^2), \quad (3)$$

where $\langle \cdot \rangle_V$ denotes a spatial average.

2 Numerical simulations

Data has been generated by direct numerical simulation of the 3D Navier-Stokes equations on a triply periodic domain of size $L_{\text{box}} = 2\pi$ in each spatial direction

$$\partial_t \mathbf{u} + \mathbf{u} \cdot \nabla \mathbf{u} = -\nabla p + \nu \Delta \mathbf{u} + \mathbf{f}, \quad (4)$$

$$\nabla \cdot \mathbf{u} = 0, \quad (5)$$

where \mathbf{u} denotes the velocity field, p is the pressure divided by the fluid density, which is constant, and ν the kinematic viscosity. The forcing \mathbf{f} is a random Gaussian process with zero mean active in the wavenumber band $k \in [0.5, 2.4]$ for the dataset HL2 while for HL1 the forcing ranges in the interval $k \in [1.0, 2.0]$. It satisfies $\nabla \cdot \mathbf{f} = 0$, and is fully helical, $\mathbf{f} = \mathbf{f}^+$. Equations (4)-(5) were stepped forwards in time using a second-order Adams-Bashforth scheme, with the viscous term treated implicitly using an integrating factor. The spatial discretisation was implemented via the standard pseudospectral method with complete dealiasing by the two-thirds rule. Further details and mean values of key observables are summarised in table 1.

id	N	E	ν	ε	L	τ	Re_λ	$\eta/10^{-3}$	k_{max}	$k_{\text{max}}\eta$	$\Delta t/\tau$	#
HL1	512	6.32	0.002	2.88	1.14	0.50	240	7.41	169	1.25	0.60	56
HL2	1024	7.26	0.001	3.33	1.12	0.50	327	4.20	340	1.43	0.60	39

Table 1: Simulation parameters and key observables, where N denotes the number of collocation points in each coordinate, E the total kinetic energy per unit volume, ν the kinematic viscosity, ε the dissipation rate, $L = (3\pi/4E) \sum_{k=1}^{k_{\text{max}}} E(k)/k$ Δk the integral scale, $\tau = L/\sqrt{2E/3}$ the large-eddy turnover time, Re_λ the Taylor-scale Reynolds number, $\eta = (\nu^3/\varepsilon)^{1/4}$ the Kolmogorov microscale, k_{max} the largest wave number after de-aliasing, Δt the amplifying interval which is calculated from the length of the averaging interval divided by the number of equispaced snapshots, and # the number of snapshots. The higher-resolved data corresponds to run 22 of Sahoo *et al.* (2015). Both datasets have been discussed in Capocci *et al.* (2023) and are available for download using the SMART-Turb portal <http://smart-turb.roma2.infn.it>.

Time series of the total kinetic energy per unit volume, $E(t) = \frac{1}{2} \langle |\mathbf{u}(\mathbf{x}, t)|^2 \rangle_V$, and the total dissipation, $\varepsilon(t) = \langle |\nabla \mathbf{u}(\mathbf{x}, t)|^2 \rangle_V$, for datasets HL1 and HL2, are presented in Fig. 1. The red points correspond to instances in time where full data cubes have been sampled.

Figure 2 shows the energy spectrum $E(k) = \frac{1}{2} \sum_{k \leq |\mathbf{k}| < k+1} |\hat{\mathbf{u}}(\mathbf{k})|^2$ averaged over the ensemble of 56 and 39 velocity-field configurations that comprise the datasets of HL1 and HL2 respectively, in raw and Kolmogorov-compensated form. The energy spectrum can be decomposed into contributions from the positively and negatively helical components of the velocity field, $E(k) = E^+(k) + E^-(k)$. In both panels of the figure, the black lines correspond to $E(k)$, the red lines to the energy spectrum of the positively helical velocity-field fluctuations, $E^+(k)$ and the blue lines to that of the negatively helical velocity-field fluctuations, $E^-(k)$. The grey-shaded area identifies the forcing range, and the horizontal dashed line, in the compensated spectra of both panels, indicates a Kolmogorov constant $C_K = 1.6$. As the forcing is positively helical, the negatively helical fluctuations must be maintained by nonlinear coupling to the positively helical fluctuations. As can be seen from the data presented in Fig. 2, the velocity field is positively helical at and near the forcing scales. In both datasets, the mirror symmetry is restored towards the end of the inertial range, around $k = 80$. Only the $E(k)$ and $E^+(k)$ scale approximately as $k^{-5/3}$, while $E^-(k)$ has a shallower slope.

3 DataBase Description

TURB-Hel database is made of files extracted from the 512³ HL1 and 1024³ HL2 simulation described in the previous section as follows:

- During the simulation we dumped the vector potential of the velocity field in fourier space every 3000 Δt simulation steps. In total we stored 56 (HL1) and 39 (HL2) configurations, we call them "cb" (from Complex B-field);

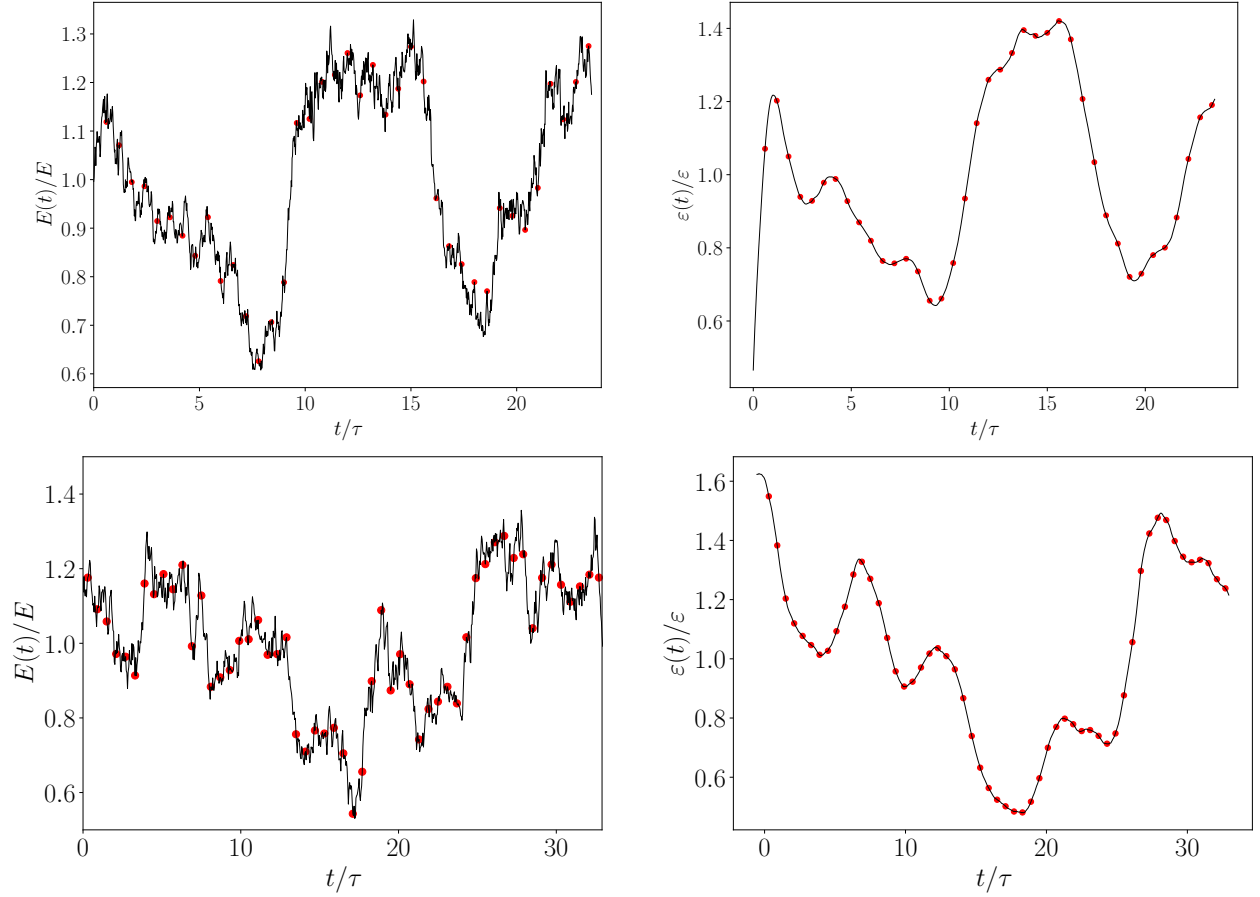


Figure 1: Time evolution of the total energy (left) and the total dissipation (right). The red dots correspond to the sampled velocity-field configurations.

Top panel: dataset HL2.

Bottom panel: dataset HL1.

- In order to recover the velocity fields, every configuration should be read using the HDF5 library, then a curl operation is needed to compute the velocity field in Fourier space.
- If the velocity field is needed in real space, a backward FFT is needed.
- In the support materials, there is a C program

```
read_cb
```

which performs all the above steps, and an accompanying README.pdf for the details on how to compile it.

The database TURB-Hel is available for download using the SMART-Turb portal at <http://smart-turb.roma2.infn.it>.

Other data-sets concerning rotating turbulence (TURB-Rot Biferale *et al.* (2020)) and Lagrangian particle under turbulence (TURB-Lagr) are already available.

Acknowledgements

This work received funding from the European Research Council (ERC) under the European Union's Horizon 2020 research and innovation programme (grant agreement No 882340).

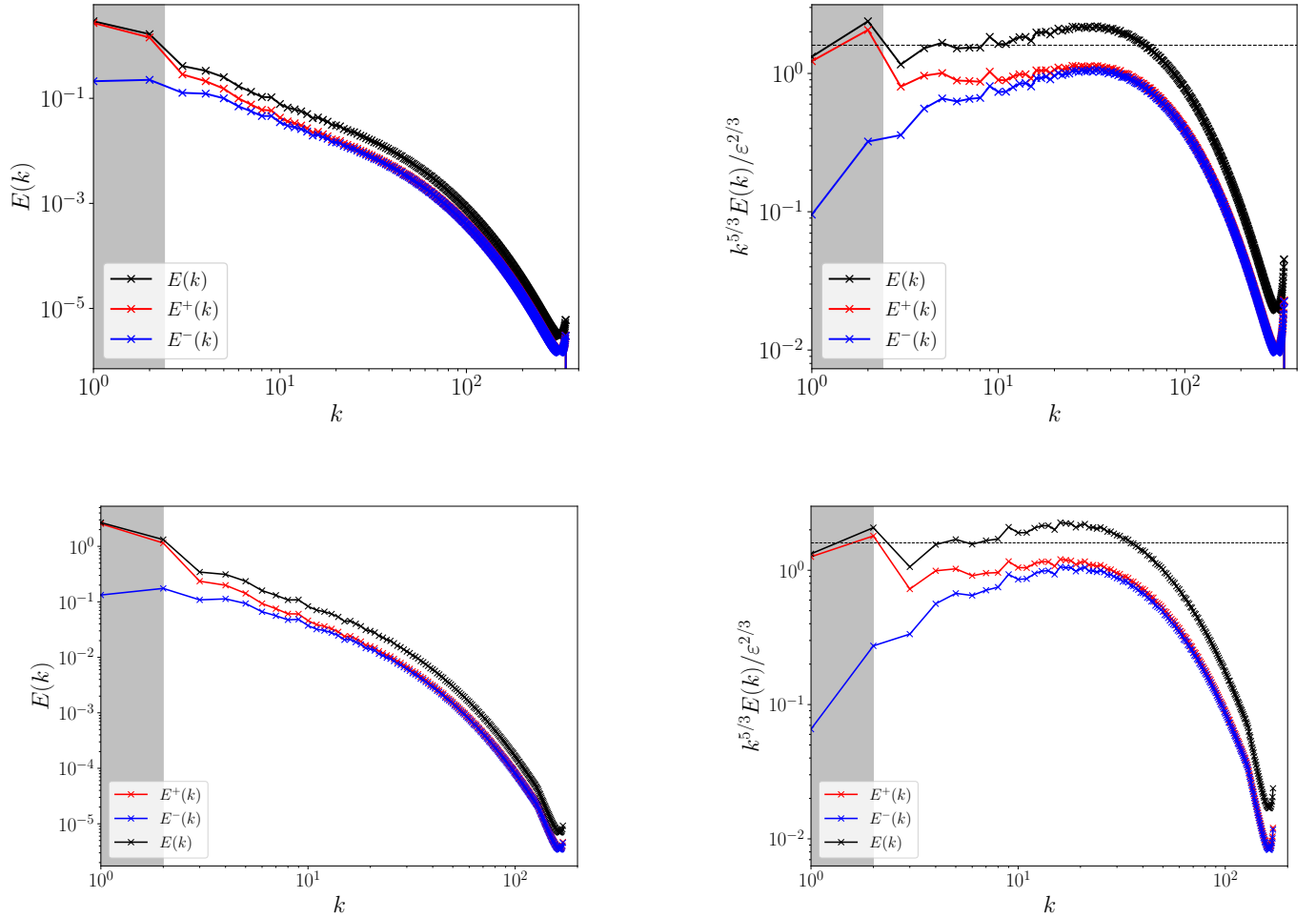


Figure 2: Time-averaged energy spectra, in raw (left) and Kolmogorov-compensated (right) form. The grey-shaded area indicates the forcing range, the positively helical component is shown in red, the negatively helical component in blue and the total energy spectrum in black.

Top panel: dataset HL2.

Bottom panel: dataset HL1: a fewer amount of wavenumbers is the consequence of the reduction in the grid point. In both datasets the dashed lines in the right panels indicate a Kolmogorov constant $C_K \approx 1.6$.

References

- ALEXAKIS, A. 2017 Helically decomposed turbulence. *Journal of Fluid Mechanics* **812**, 752–770.
- ALEXAKIS, A. & BIFERALE, L. 2018 Cascades and transitions in turbulent flows. *Physics Reports* **767**, 1–101.
- BIFERALE, L., BONACCORSO, F., BUZZICOTTI, M. & DI LEONI, P. C. 2020 Turb-rot. a large database of 3d and 2d snapshots from turbulent rotating flows. *arXiv preprint arXiv:2006.07469* .
- BIFERALE, L., MUSACCHIO, S. & TOSCHI, F. 2012 Inverse energy cascade in three-dimensional isotropic turbulence. *Physical review letters* **108** (16), 164501.
- BIFERALE, L, MUSACCHIO, STEFANO & TOSCHI, F 2013 Split energy–helicity cascades in three-dimensional homogeneous and isotropic turbulence. *Journal of Fluid Mechanics* **730**, 309–327.
- CAPOCCI, D., JOHNSON, P. L., OUGHTON, S., BIFERALE, L. & LINKMANN, M. 2023 New exact betchov-like relation for the helicity flux in homogeneous turbulence. *Journal of Fluid Mechanics* **963**, R1.
- KRAICHNAN, ROBERT H 1973 Helical turbulence and absolute equilibrium. *Journal of Fluid Mechanics* **59** (4), 745–752.
- MOFFATT, H K. 2014 Helicity and singular structures in fluid dynamics. *Proceedings of the National Academy of Sciences* **111** (10), 3663–3670.
- SAHOO, G., BONACCORSO, F. & BIFERALE, L. 2015 Role of helicity for large- and small-scale turbulent fluctuations. *Phys. Rev. E* **92**, 051002.
- WALEFFE, F. 1992 The nature of triad interactions in homogeneous turbulence. *Physics of Fluids A: Fluid Dynamics* **4** (2), 350–363.